

# Synthesis and Characterization of Tetraborate Pillared Hydrotalcite

Liansheng Li,<sup>\*,†</sup> Shujie Ma,<sup>†</sup> Xinsheng Liu,<sup>\*,†,||</sup> Yong Yue,<sup>‡</sup> Jianbin Hui,<sup>†</sup> Ruren Xu,<sup>†</sup> Yumin Bao,<sup>§</sup> and J. Rocha<sup>⊥</sup>

Department of Chemistry, Jilin University, Changchun, The People's Republic of China; Wuhan Institute of Physics, Wuhan, The People's Republic of China; Department of Chemistry, Inner-Mongolia National Teachers College, Inner-Mongolia, The People's Republic of China; and Department of Chemistry, University of Aveiro, 3800 Aveiro, Portugal

Received July 12, 1995. Revised Manuscript Received October 23, 1995<sup>⊗</sup>

Hydrothermal synthesis of tetraborate,  $B_4O_5(OH)_4^{2-}$ , -pillared hydrotalcites was investigated, and an efficient way of preparing them was found. The structures of the pillared materials were characterized using a combination of techniques such as powder X-ray diffraction, FT-IR,  $^{11}B$  and  $^{27}Al$  MAS NMR, DTA/TGA, and chemical analysis. The results show that the structure of the coprecipitate is important in controlling the formation of  $B_4O_5(OH)_4^{2-}$ -pillared hydrotalcites. With a slurrylike precipitate, a more ordered structure of the pillared hydrotalcite is obtained, while with a wet cakelike precipitate, a disordered structure of the pillared hydrotalcite is formed. The tetraborate anions in the interlayer space orient with their tetrahedral  $BO_4$  linkage perpendicular to the sheets of hydrotalcite. The tetraborate pillared material has a chemical composition of  $[Mg_{0.70}Al_{0.30}(\text{OH})_2][B_4O_5(OH)_4]_{0.15}\cdot H_2O$  and a surface area of  $\sim 47 \text{ m}^2/\text{g}$ .

## Introduction

Hydrotalcite-like anionic clays are a family of interesting materials with many practical applications as catalysts, catalyst supports, ion exchangers,<sup>1</sup> and composite materials.<sup>2</sup> Natural hydrotalcite,  $Mg_6Al_2(OH)_{16}CO_3\cdot 4H_2O$ , structurally similar to brucite,  $Mg(OH)_2$ , is composed of sheets of edge-sharing  $Mg(OH)_6$  and  $Al(OH)_6$  octahedra. Due to isomorphous substitution of  $Al^{3+}$  for  $Mg^{2+}$ , the sheets are positively charged and stacked on top of each other and held together by charge-balancing anions, normally  $CO_3^{2-}$ , and/or hydrogen bonding. The  $Mg^{2+}$  and  $Al^{3+}$  in the sheets can also be isomorphously substituted by other metal ions having two or three positive charges and the  $CO_3^{2-}$  in the interlayer space by other inorganic and organic anions, forming new hydrotalcite-like materials. The general formula can be described as  $[M_{1-x}^{2+}M_x^{3+}(OH)_2]^{x+}A_{x/n}^{n-}\cdot mH_2O$ , where M denotes metal ions, A denotes exchangeable anions with valence n, and x is within 0.17–0.33. Recently Cavani et al.<sup>1</sup> have reviewed the synthesis, properties, and applications of hydrotalcite and hydrotalcite-like materials.

The intercalation and pillaring of hydrotalcite-like materials are of considerable current interest in the search for advanced materials, particularly, by using polyacid anions as the pillaring agents. However, it is not an easy task to directly synthesize hydrotalcite-like

materials with large inorganic anions. The normally employed method involves the use of previously prepared hydrotalcite as a precursor followed by ion exchange with the corresponding anions under certain conditions. In this way Woltermann<sup>3</sup> prepared heteropolyacid pillared hydrotalcite materials using hydrotalcite- $NO_3^-$  as a precursor. Recently Drezdzon<sup>4</sup> has successfully synthesized hydrotalcites containing large inorganic compounds using long-chain organic anion intercalated hydrotalcites as precursors. Narita et al.<sup>5</sup> took advantage of the "memory effect" of the hydrotalcite solid solutions and successfully synthesized heteropolyacid-containing hydrotalcites. Although some success has been achieved by this method, the materials obtained suffer from low crystallinity, incomplete anion exchange, and instability of the polyacid with subsequent ion exchange. Due to these reasons, work is still needed to improve the preparation method. Very recently, Bhattacharyya et al.<sup>6</sup> have successfully synthesized triborate-pillared hydrotalcite under  $N_2$  and Cheng and Lin<sup>7</sup> prepared tetraborate-pillared hydrotalcite-like materials via ion exchange with  $(NH_4)_2B_4O_7$ , using the adipate–hydrotalcite as a precursor.

In this paper, we report an effective method for the hydrothermal synthesis of tetraborate anion pillared hydrotalcites, and the results of studies on the structures and physicochemical properties of the products.

## Experimental Section

**Chemicals.**  $Mg(NO_3)_2\cdot 6H_2O$  (A.R.) was purchased from Shenyang First Chemical Reagent Plant, Shenyang, China,

(3) Woltermann, G. M. U.S. Patent 4,454,244.

(4) Drezdzon, M. A. *Inorg. Chem.* **1988**, *27*, 4628.

(5) Narita, E.; Kaviratna, P.; Pinnavaia, T. J. *Chem. Lett.* **1991**, 805.

(6) Bhattacharyya, A.; Hall, D. B. *Inorg. Chem.* **1992**, *31*, 3869.

(7) Cheng, S.; Lin, J.-T. In *Expanded Clays and Other Microporous Solids*; Occhipi, M. L., Robson, H., Eds.; van Nostrand Reinhold: New York, 1992; p 170.

<sup>†</sup> Jilin University.

<sup>‡</sup> Wuhan Institute of Physics.

<sup>§</sup> Inner-Mongolia National Teachers College.

<sup>⊥</sup> University of Aveiro.

\* To whom correspondence should be addressed.

\*\* Present address: Department of Chemistry and Biochemistry, University of Notre Dame, Notre Dame, IN 46556.

⊗ Abstract published in *Advance ACS Abstracts*, December 1, 1995.

(1) Cavani, F.; Trifiro, F.; Vaccari, A. *Catal. Today* **1991**, *11*, 173.

(2) The applications of this aspect of hydrotalcite are rather new, and many patents have been reported in *Chemical Abstracts* in very recent years.

$\text{Al}(\text{NO}_3)_3 \cdot 9\text{H}_2\text{O}$  (A.R.) and  $\text{NaOH}$  (A.R.) from Beijing Chemical Plant, Beijing, China, and  $\text{Na}_2\text{B}_4\text{O}_5(\text{OH})_4 \cdot 8\text{H}_2\text{O}$  was obtained from Jilin University Chemical Reagent Plant, Changchun, China.

**Synthesis of  $\text{B}_4\text{O}_5(\text{OH})_4^{2-}$ -Containing Hydrotalcite.**  $\text{Mg}(\text{NO}_3)_2 \cdot 6\text{H}_2\text{O}$  (3.85 g) and  $\text{Al}(\text{NO}_3)_3 \cdot 9\text{H}_2\text{O}$  (2.81 g) were dissolved into 40 mL water, and then a 2 N aqueous solution of  $\text{NaOH}$  was added dropwise to the above solution under stirring to make a coprecipitate. The final pH of the solution was controlled to be 9. After separation of the precipitate from the liquid, the precipitate was washed with deionized water three times. During the separation and washing, some liquid was left on the top of the precipitate. The precipitate together with the residual water was then dispersed into a hot aqueous solution of  $\text{Na}_2\text{B}_4\text{O}_5(\text{OH})_4 \cdot 8\text{H}_2\text{O}$  (20 mL, 0.5 M). The pH of the slurry was also controlled to be 9. The slurry was transferred into a Teflon-lined autoclave and heated at 100 °C for 20 h. The product was separated by filtration, washed with deionized water, and dried in air.

**Instruments.** Powder X-ray diffraction was carried out on a Kagaku D/Max-IIIA X-ray powder diffractometer operating at 30 kV and 20 mA with  $\text{Cu K}\alpha$  radiation ( $\lambda = 1.5418 \text{ \AA}$ ) and on a Philips diffractometer automated with an ADP 3520 system operating at 40 kV and 30 mA with also  $\text{Cu K}\alpha$  radiation. FT-IR spectra were recorded on a Mattson Galaxy 5020-FTIR spectrometer. The KBr pellet method was used. Differential thermal analysis (DTA) and thermal gravimetric analysis (TGA) were performed on Perkin-Elmer DTA1700/TGA7 thermal analysis instruments. The heating speed was 10°/min with a  $\text{N}_2$  gas flow rate of 20 mL/min.  $^{11}\text{B}$  magic-angle spinning NMR (MAS NMR) spectra were recorded on a Bruker MLS-400 spectrometer with a spinning speed 8 kHz. Solid  $\text{KBF}_3$  was taken as a reference.  $^{27}\text{Al}$  MAS NMR spectra were measured on a Varian XL-200 NMR spectrometer with a spinning speed 4 kHz. A solution of  $\text{Al}(\text{NO}_3)_3$  was taken as a standard. The surface area measurements of the samples were performed using the standard BET method. The sample pellets were made and crushed to a particle size of 40–60 mesh. The samples were then heated at 150 °C for 4 h under vacuum ( $10^{-4}$  Torr). The adsorption of  $\text{N}_2$  was carried out at 77 K. Chemical analysis was carried out on a Jarrell-Ash Mark-II inductively coupled Ar plasma atomic emission spectrometer.

## Results and Discussion

We have successfully synthesized tetraborate,  $\text{B}_4\text{O}_5(\text{OH})_4^{2-}$ , pillared hydrotalcites under hydrothermal conditions at 100 °C. The synthesis was performed by making a coprecipitate of  $\text{Mg}(\text{OH})_2$  and  $\text{Al}(\text{OH})_3$  from a mixed aqueous solution of  $\text{Mg}(\text{NO}_3)_2 \cdot 6\text{H}_2\text{O}$  and  $\text{Al}(\text{NO}_3)_3 \cdot 9\text{H}_2\text{O}$  with an aqueous solution of  $\text{NaOH}$ , followed by separation of the precipitate from the liquid, washing with deionized water, and redispersing it into a hot aqueous solution of  $\text{Na}_2\text{B}_4\text{O}_5(\text{OH})_4 \cdot 8\text{H}_2\text{O}$  (60 °C). The main difference in this method compared to those reported in the literature<sup>1,3–7</sup> is the use of wet cakelike or slurrylike coprecipitates of  $\text{Al}(\text{OH})_3$  and  $\text{Mg}(\text{OH})_2$  as precursors. The precipitate was washed with water and filtered by vacuum pumping either to a wet “cake” (no liquid water left on the top of the precipitate) or to a slurry (with a small amount of water left on the top of the precipitate). The washing was carried out three times in the same way.

It was found that with the wet cakelike precipitate, the crystallization was slow and took more than 30 days to complete, but with the slurrylike precipitate, the crystallization was fast and completed only in about 1 day. For comparison, typical powder X-ray diffraction patterns of the products obtained from these two methods are given in Figure 1. The top pattern in the figure is from the product of the slurry method after 18 h crystallization, while the bottom one is from that with

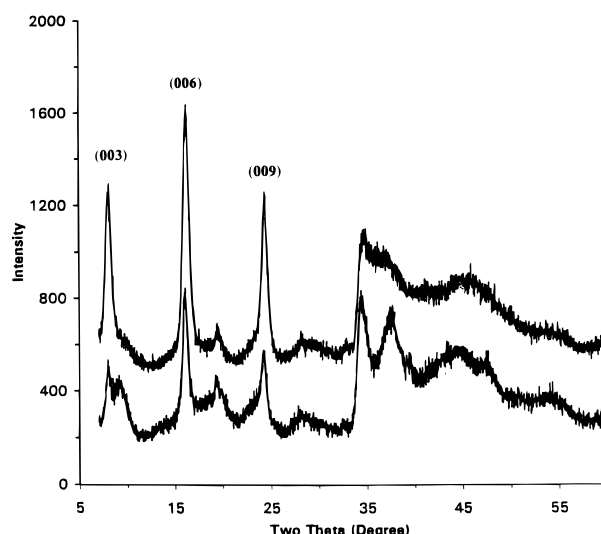


**Figure 1.** X-ray diffraction patterns of the products obtained from the wet cake method and the slurry method. The top pattern is the product of the slurry method obtained after 20 h crystallization and the bottom pattern is that of the wet cake method obtained after 30 days crystallization.

the wet cake method after 30 days crystallization. The XRD patterns clearly show that the slurry method is much better than the wet cake method. The significant difference in products obtained from these two methods suggests that the structure of the precipitate is a key factor controlling the formation of tetraborate pillared hydrotalcite.

The phenomenon observed here can be rationalized as follows: Initially the coprecipitate of  $\text{Mg}(\text{OH})_2$  and  $\text{Al}(\text{OH})_3$  is cottonlike and loose. The precipitate will exhibit a hydrotalcite structure if it is separated from the liquid, washed with water, and dried. The strong interactions between the charges of the sheets and the anions in the interlayer space prevent intercalation of the hydrotalcite by the anions  $\text{B}_4\text{O}_5(\text{OH})_4^{2-}$ . Due to this reason, no borate-pillared hydrotalcite could be obtained from a direct ion exchange of the dried hydrotalcite.<sup>7</sup> The structure of the wet cakelike precipitate is similar to that of the dried hydrotalcite, and its interlayer space is difficult to be reopened by the  $\text{B}_4\text{O}_5(\text{OH})_4^{2-}$  anions, thus preventing pillaring, while the slurrylike precipitate maintains the separation of the sheets and allows the anions to enter the interlayer space to organize, leading to the formation of pillared hydrotalcite. Consistent with this explanation are the highly disordered structures of the products in the wet cake case, as shown by the very broad peaks in their XRD patterns (Figures 1 and 2), and the successful pillaring of hydrotalcites with large inorganic anions with the help of long chain organic anions as interlayer space “opener”.<sup>4</sup> It is therefore concluded that the protection of the structure of the cottonlike precipitate in the slurry method facilitates pillaring during the crystallization.

It is also seen from Figure 1 that the first peak at ~8° ( $2\theta$ ) of the product obtained using the slurry method is composed of only one peak, while that of the product obtained using the wet cake method is a doublet, one of the doublet peaks occurs at a position similar to that obtained using the slurry method and the other is a broad peak centered at ~9°. Because both patterns have the same peaks at 16° and 24° which correspond, respectively, to the (006) and (009) diffractions, the peak at 8° is due to the (003) diffraction and the peak at ~9°

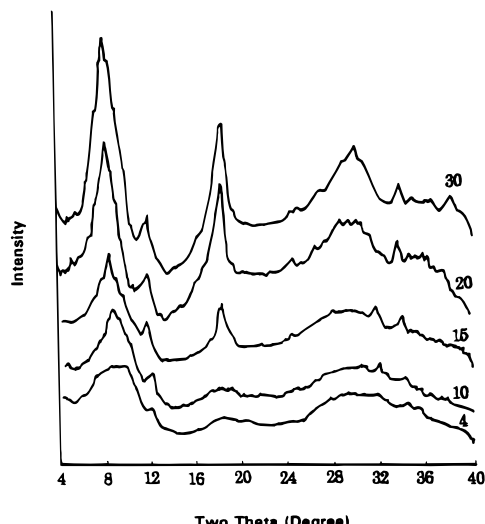


**Figure 2.** Monitoring the crystallization process with the wet cake method by XRD diffraction. The numbers indicate the crystallization time in days.

originates from a poorly pillared hydrotalcite. A well-resolved peak at  $\sim 9^\circ$  is not generally observed, in most cases, only a very broad peak around  $8.5^\circ$  ( $2\theta$ ) was obtained, corresponding to an overlapping of these two peaks. Similar phenomena were also observed for the vanadate-exchanged hydrotalcites by Ulibarri et al.<sup>8</sup> and for the polyoxometallate-pillared hydrotalcites by Narita et al.<sup>5</sup> and Wang et al.<sup>9</sup> These authors proposed the presence of other phases in their samples.

To understand the nature of the peak at  $\sim 9^\circ$  in the powder XRD pattern of the product from the wet cake method, the crystallization process of the wet cake method was followed by using the XRD technique (Figure 2). The XRD peaks increase in intensity and shift toward a smaller  $2\theta$  angle as the crystallization proceeds. The (003) peak (the peak with the smallest  $2\theta$  angle) and other peaks (Figure 2) are very broad for the products obtained after a short time of crystallization. As the crystallization proceeds, the peaks are shifted and become narrower. The broad (003) peak shifts toward  $8^\circ$  and no longer changes after 20 days crystallization. From these changes, it is clear that, the broad peaks originate from the disordered nature of the pillaring, not from a separate "impurity" phase. The ordering is improved at the expense of the disordered phase as the crystallization proceeds. When the ordered phase becomes dominant, the peaks no longer shift. Contamination by  $\text{CO}_2$  in the atmosphere is present during the sample preparation, which gives a weak peak at  $\sim 11^\circ$  in the XRD patterns (Figure 2), consistent with the size of  $\text{CO}_3^{2-}$  anions,  $2.8 \text{ \AA}$ .

To know how the  $\text{B}_4\text{O}_5(\text{OH})_4^{2-}$  anions orient in the interlayer space, the distance of the interlayer space and the geometric configuration of the tetraborate anion were calculated using the XRD pattern and the Spartan computer program (AM1),<sup>10</sup> respectively. The  $8^\circ 2\theta$  corresponds to a  $d$  spacing of  $11.0 \text{ \AA}$ . The distance of the interlayer space is therefore estimated to be  $6.2 \text{ \AA}$  by subtraction of the sheet thickness of hydrotalcite,  $4.8$

(8) Ulibarri, M.-A.; Labajos, F. M.; Rivea, V.; Trulillano, R.; Kaguny, W.; Jones, W. *Inorg. Chem.* **1994**, *33*, 2592.

(9) Wang, J.; Tiam, Y.; Wang, R.-C.; Clearfield, A. *Chem. Mater.* **1992**, *4*, 1276.

(10) Hehre, W. J.; Burke, L. D.; Shusterman, A. J. *SPARTAN, Version 3.0*, Wavefunction, Inc., 1993.

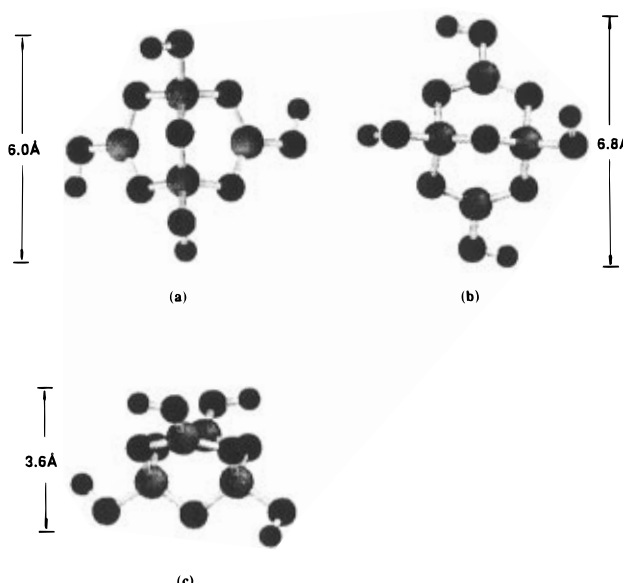


**Figure 3.** Schematic drawing of  $\text{B}_4\text{O}_5(\text{OH})_4^{2-}$  anion along different projections after energy minimization and geometry optimization using the Spartan program. The large balls are boron, the medium balls oxygen, and the small balls hydrogen.

**Table 1. Effects of pH on the Products Obtained<sup>a</sup>**

pH	7	8	9	10	11
product	Am	B-HT	B-HT	B-HT + Am	HT-OH <sup>-</sup> + Am

<sup>a</sup> Am denotes amorphous materials, B-HT denotes  $\text{B}_4\text{O}_5(\text{OH})_4^{2-}$ -pillared hydrotalcite. HT-OH<sup>-</sup> is the hydrotalcite with OH<sup>-</sup> as a charge-balancing anion.

$\text{\AA}$ , from this value, i.e.,  $11.0 - 4.8 = 6.2 \text{ \AA}$ . The dimensions of the tetraborate anion after energy minimization and geometry optimization using the Spartan program are given in different projections in Figure 3. The sizes of the molecule along different projections were estimated from the summation of the distance of the two outermost H atoms and their covalent radii,<sup>11</sup> i.e.,  $d_{\text{H-H}} + 0.3 \times 2 \text{ \AA}$ . Comparing the dimensions with the distance of the interlayer space of the samples shows that the tetraborate anions are oriented in such a way that the tetrahedral  $\text{BO}_4$  linkage of the molecule is perpendicular to the hydrotalcite sheets (see the configuration (a) in Figure 3). This kind of orientation of  $\text{B}_4\text{O}_5(\text{OH})_4^{2-}$  in the interlayer space of hydrotalcite reflects the preferred interactions of the more negatively charged tetrahedral  $\text{BO}_4$  of the molecules with the positive charge on the sheets. The other orientations in the interlayer space are only possible at the earlier stages of the crystallization as exemplified by the very broad peaks in the XRD pattern (see Figure 2). Due to the unfavorable interactions with the negative charges of the tetraborate anion, these orientations are energetically unstable and tend to adjust as the crystallization proceeds.

The pH of the slurry is important for the formation of  $\text{B}_4\text{O}_5(\text{OH})_4^{2-}$ -pillared hydrotalcite. Table 1 shows the effects of the slurry pH on the product obtained. The most preferred pH for the formation of  $\text{B}_4\text{O}_5(\text{OH})_4^{2-}$ -pillared hydrotalcite is within 8–9. Below 8, amorphous materials are obtained, while above 9, the crystallization is incomplete. When the pH is 11, hydrotalcite with OH<sup>-</sup> as a charge-balancing anion is formed together with amorphous phases. This parallels the stability of

(11) Atkins, P. W. *Physical Chemistry*, 2nd ed.; W. H. Freeman: San Francisco, CA, 1982; p 756.

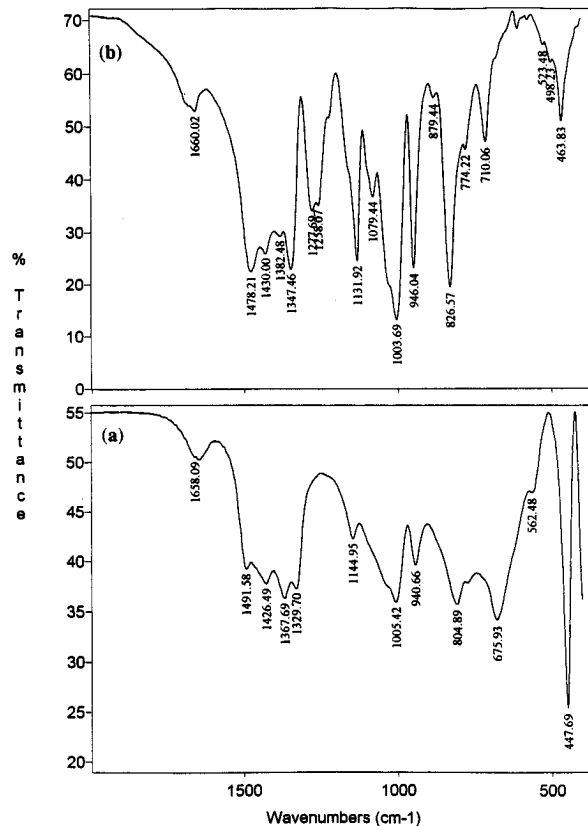


**Figure 4.** FT-IR spectra of  $\text{B}_4\text{O}_5(\text{OH})_4^{2-}$ -pillared hydrotalcite (a) and the solid  $\text{Na}_2\text{B}_4\text{O}_5(\text{OH})_4 \cdot 8\text{H}_2\text{O}$  (b).

tetraborate anion with pH. Similar pH effects have also been observed by Bhattacharyya and Hall<sup>6</sup> for their triborate-pillared hydrotalcites.

Figure 4 shows the infrared spectra of the  $\text{B}_4\text{O}_5(\text{OH})_4^{2-}$ -pillared hydrotalcite obtained from the slurry method and solid  $\text{Na}_2\text{B}_4\text{O}_5(\text{OH})_4 \cdot 8\text{H}_2\text{O}$ . The solid  $\text{Na}_2\text{B}_4\text{O}_5(\text{OH})_4 \cdot 8\text{H}_2\text{O}$  is included for comparison. Table 2 summarizes the data from the infrared spectra and their assignments, following the data from the literature.<sup>12–15</sup> The 1492, 1426, 1368, and 1330 cm<sup>-1</sup> bands of the pillared hydrotalcite are assigned to  $\nu_3 \text{BO}_3$  stretching and B–OH in-plane bending vibrations, the 941 cm<sup>-1</sup> band to  $\nu_1 \text{BO}_3$  stretching and B–OH in-plane bending vibrations, the 805 cm<sup>-1</sup> band to  $\nu_2 \text{BO}_3$  stretching vibrations, and those at 1146 and 1005 cm<sup>-1</sup> to  $\nu_3 \text{BO}_4$  stretching and B–OH in-plane bending vibrations. The bands with wavenumbers smaller than 800 cm<sup>-1</sup> are assigned to the hydrotalcite lattice vibrations. From Figure 4 and Table 2 it is obvious that (1) intercalation of  $\text{B}_4\text{O}_5(\text{OH})_4^{2-}$  in hydrotalcite indeed takes place, which is consistent with the XRD results given above, (2) the similarity of the corresponding vibration bands to those of the  $\text{Na}_2\text{B}_4\text{O}_5(\text{OH})_4 \cdot 8\text{H}_2\text{O}$  indicates that the  $\text{B}_4\text{O}_5(\text{OH})_4^{2-}$  anions intercalated retain their structures as the original anions, (3) the shifts and intensity changes reflect the difference in environment experienced by the anions in the salt and in the product, the vibrations of  $\text{BO}_3$  being more “relaxed” (lengthening the B–O bond) and those of the  $\text{BO}_4$  more “stressed” (shortening the

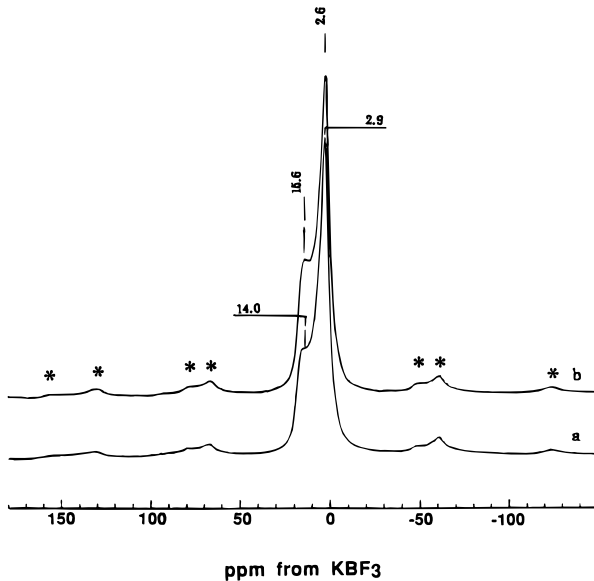


**Figure 5.**  $^{11}\text{B}$  MAS NMR spectra of  $\text{B}_4\text{O}_5(\text{OH})_4^{2-}$ -pillared hydrotalcite before (a) and after (b) calcination at 300 °C for 3 h.

**Table 2. Infrared Spectroscopic Data and Their Assignments of the  $\text{B}_4\text{O}_5(\text{OH})_4^{2-}$ -Pillared Hydrotalcite and  $\text{Na}_2\text{B}_4\text{O}_5(\text{OH})_4 \cdot 8\text{H}_2\text{O}$**

B-HT (cm <sup>-1</sup> )	$\text{Na}_2\text{B}_4\text{O}_5(\text{OH})_4 \cdot 8\text{H}_2\text{O}$ (cm <sup>-1</sup> )	$\Delta\nu$ (cm <sup>-1</sup> )	assignments
1492	1478	14	$\nu_3 \text{BO}_3$ , BOH
1426	1430	-4	$\nu_3 \text{BO}_3$ , BOH
1368	1382	-14	$\nu_3 \text{BO}_3$ , BOH
1330	1347	-17	$\nu_3 \text{BO}_3$ , BOH
	1278, 1258		BOH
1145	1132	13	$\nu_3 \text{BO}_4$ , BOH
	1079		$\nu_3 \text{BO}_4$ , BOH
1005	1004	1	$\nu_3 \text{BO}_4$ , BOH
941	946	-5	$\nu_1 \text{BO}_3$
805	827	-22	$\nu_2 \text{BO}_3$
	774, 710		
676			HT lattice
562			HT lattice
	464		
448			HT lattice

B–O bond). This is consistent with the orientation of  $\text{B}_4\text{O}_5(\text{OH})_4^{2-}$  proposed from the XRD results.

Figure 5 shows the  $^{11}\text{B}$  MAS NMR spectra of the  $\text{B}_4\text{O}_5(\text{OH})_4^{2-}$ -pillared hydrotalcite obtained from the slurry method and the sample after calcination at 300 °C for 3 h. Two bands are observed with chemical shifts at 2.9 and 14.0 ppm, respectively. The band at 2.9 ppm is assigned to the tetrahedrally coordinated boron, while that at 14.0 ppm to the trigonally coordinated boron.<sup>16</sup> Due to the overlapping of the signals of these two types of boron in the  $\text{B}_4\text{O}_5(\text{OH})_4^{2-}$  anion, it is not straightforward to obtain the intensity ratio of the two kinds of boron from a simple deconvolution of the spectrum. The previously reported  $^{11}\text{B}$  MAS NMR spectra of boron-containing zeolites,<sup>16</sup> boron-glass,<sup>17</sup> and triborate-pillared hydrotalcites<sup>6</sup> have shown that the trigonally coordinated boron has a higher second-order quadrupolar interaction exhibiting “doublet” patterns, while the

(12) Nakanish, K.; Solomon, P. H. *Infrared Absorption Spectroscopy*, 2nd ed.; London, 1977; p 55.

(13) Socrates, G. *Infrared Characteristic Group Frequencies*; John Wiley & Sons: New York, 1980; p 131.

(14) Hernandez-Moreno, M. J. *Phys. Chem. Miner.* **1985**, *12*, 34.

(15) Devi, S. A.; Philip, D. Aruldas, G. *J. Solid State. Chem.* **1994**, *113*, 157.

(16) Engelhardt, G.; Michel, D. *High-Resolution Solid-State NMR of Silicates and Zeolites*; John Wiley & Sons: New York, 1987, p 332 and references therein.

(17) Fyfe, C. A.; Bemis, L.; Clark, H. C.; Davies, J. A.; Gobbi, G. C.; Hartman, J. S.; Hayes, P. J.; Wasylshen, R. E. *Inorganic Chemistry: Toward the 21st Century*; American Chemical Society: Washington DC, 1983; p 405.

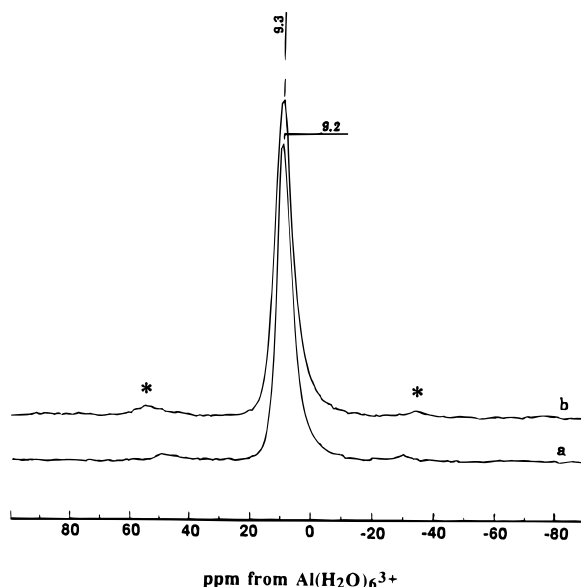


**Figure 6.**  $^{27}\text{Al}$  MAS NMR spectra of  $\text{B}_4\text{O}_5(\text{OH})_4^{2-}$ -pillared hydrotalcite before (a) and after (b) calcination at  $300^\circ\text{C}$  for 3 h.

tetrahedrally coordinated boron exhibits relatively narrow single lines. On the basis of these facts, the deconvolution of the  $^{11}\text{B}$  MAS NMR spectrum in Figure 4 gives a 1:1 intensity ratio of tetrahedral to trigonal boron, which is consistent with the structure of  $\text{B}_4\text{O}_5(\text{OH})_4^{2-}$ . This spectral interpretation is also supported by chemical analysis of the sample (see below).

Calcination of the sample at  $300^\circ\text{C}$  for 3 h shifts the tetrahedral boron band from 2.9 to 2.6 ppm and alters the relative intensity ratio of tetrahedral to trigonal B to 0.85:1. The change of the relative intensity indicates that about 8% of the tetrahedrally coordinated boron is converted to trigonally coordinated boron by calcination. The conversion of tetrahedrally coordinated boron to trigonally coordinated boron upon calcination is a common phenomenon observed in boron-containing zeolites.<sup>16</sup>

The  $^{27}\text{Al}$  MAS NMR spectra of the samples before and after calcination at  $300^\circ\text{C}$  for 3 h are given in Figure 6. Only one peak at a chemical shift of 9.2 ppm is observed and is assigned to octahedrally coordinated Al in the hydrotalcite sheets. After calcination, no tetrahedrally coordinated Al is observed. The changes in chemical shift of the octahedral Al is small; the band only becomes broader. The band width at half maximum is increased by 156 Hz from 1032 to 1188 Hz. This suggests that the interactions between the Al in the sheets and the B of the pillar become stronger after dehydroxylation.

Figure 7 gives the DTA and TGA curves of the tetraborate-pillared hydrotalcite sample (a product of the slurry method). For the DTA curve, four endothermic peaks at 155, 220, 340, and  $540^\circ\text{C}$  and one exothermic peak at  $680^\circ\text{C}$  are observed. The endothermic peaks correspond to dehydration of the sample ( $155^\circ\text{C}$ ), and dehydroxylation of the hydrotalcite sheets and  $\text{B}_4\text{O}_5(\text{OH})_4^{2-}$  anion (220, 340, and  $540^\circ\text{C}$ ), while the exothermic peak ( $680^\circ\text{C}$ ) corresponds to the complete lattice collapse and a phase transition.<sup>7,18</sup> The TGA data parallel well the DTA results, reflecting the

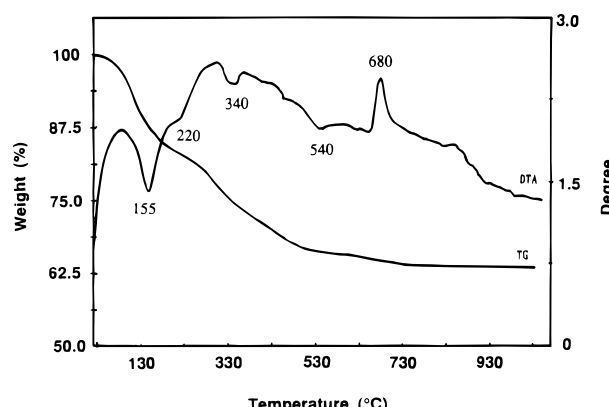


**Figure 7.** DTA and TGA curves of  $\text{B}_4\text{O}_5(\text{OH})_4^{2-}$ -pillared hydrotalcite.

corresponding weight loss at each stage. From this curve,  $\sim 17\%$  of water is present in the sample, and  $\sim 19\%$  of the weight loss is due to the dehydroxylation of the hydrotalcite sheets and the  $\text{B}_4\text{O}_5(\text{OH})_4^{2-}$  anions.

Chemical analysis of the tetraborate-pillared hydrotalcite sample gives Mg 21.5%, Al 10.3%, and B 7.1%. Together with the weight loss of dehydration, the chemical composition of the sample is  $[\text{Mg}_{0.70}\text{Al}_{0.30}(\text{OH})_2] \cdot [\text{B}_4\text{O}_5(\text{OH})_4]_{0.15} \cdot \text{H}_2\text{O}$ . It is clear that a complete charge balancing is achieved between the positive charge of the hydrotalcite sheets and the negative charge of the tetraborate anions. The balancing of charge confirms that no structural change of the tetraborate anions occurs during the crystallization.

The BET measurements of the tetraborate-pillared hydrotalcite samples before and after calcination at  $300^\circ\text{C}$  gave the surface areas of 47.0 and 46.3  $\text{m}^2/\text{g}$ , respectively. The same surface area of the sample before and after calcination indicates that the structure of the tetraborate-pillared hydrotalcite remains.

## Conclusions

The results presented here demonstrate that the structure of the coprecipitate of  $\text{Mg}(\text{OH})_2$  and  $\text{Al}(\text{OH})_3$  is important for the hydrothermal synthesis of tetraborate-pillared hydrotalcite. With a slurry-like coprecipitate, more ordered pillared products are obtained in shorter time ( $\sim 24$  h) compared to those with a wet cakelike coprecipitate ( $>30$  days). The  $\text{B}_4\text{O}_5(\text{OH})_4^{2-}$  in the products retains its structure and orients with its tetrahedral  $\text{BO}_4$  linkage perpendicular to the hydrotalcite sheets. The chemical composition of the product is  $[\text{Mg}_{0.70}\text{Al}_{0.30}(\text{OH})_2] \cdot [\text{B}_4\text{O}_5(\text{OH})_4]_{0.15} \cdot \text{H}_2\text{O}$ . The balancing of the charge between the sheets and the tetraborate anions follows the concept that the charge of the hydrotalcite sheets controls the amount of the anions intercalated.

**Acknowledgment.** The authors wish to thank China National Natural Science Foundation for financial support of this work.